European Journal of Immunology

Functional engraftment of human peripheral T and B cells and sustained production of autoantibodies in NOD/LtSzscid/IL-2R$\gamma^{-/-}$ mice

Yuki Ishikawa, Takashi Usui, Aoi Shiomi, Masakazu Shimizu, Kosaku Murakami and Tsuneyo Mimori

Department of Rheumatology and Clinical Immunology, Graduate School of Medicine, Kyoto University, Kyoto, Japan

NOD/LtSzscid/IL-2R$\gamma^{-/-}$ (NSG) mice have advantages in establishing humanized mouse models. However, transferring human PBMCs into these mice often causes lethal GVH disease. In this study, we discovered an improved method for the engraftment of normal or pathological human PBMCs into NSG mice and examined the subsequent induction of specific immune responses. We sequentially transferred human CD4$^+$ memory T (Tm) and B cells obtained from PBMCs of healthy adults or patients with autoimmune diseases into NSG mice. Removing naïve CD4$^+$ T cells from the transferred PBMCs allowed successful engraftment without lethal GVH disease. The transferred Tm cells were found to reside mainly in the spleen and the lymphoid nodules, where they expressed MHC class II molecules and produced cytokines, including IL-21. Surprisingly, the transferred B cells were also well maintained in the lymphoid organs, underwent de novo class-switch recombination, and secreted all isotypes of human Igs at significant levels. Moreover, transferring patient-derived Tm and B cells resulted in sustained production of IgM-rheumatoid factor and antiaminoacyl transfer RNA synthetase Abs in these mice. These results suggest that transfer of Tm and B cells derived from human PBMCs into NSG mice could be a useful method for the study of human autoimmune mechanisms.

Keywords: Animal models · Antibodies · Autoimmunity · Immune responses · Memory cells

Additional supporting information may be found in the online version of this article at the publisher's web-site

Introduction

It has been difficult to reconstitute functional human immune systems in experimental mice primarily because of species specificity. NOD/Shi-scid/IL-2R$\gamma^{-/-}$ (NOG) or NSG mice are severely immunodeficient because of their SCID mutation and IL-2 receptor common γ-chain deficiency [1, 2]. Due to their high engraftment rate with human-derived tissues, these mice have been useful for studying xenotransplantation [3, 4] and human immune responses against viral infections [5–7]. Successful reconstruction of human immune systems in NOG mice was first accomplished by transferring HSCs [8]. Although multiple lineages of human lymphocytes could develop in situ [9, 10], immune responses were still limited in these mice [9, 11, 12]. Indeed, several immunization challenges to the humanized NOG/NSG mice showed poor IgG production, which suggested that the interactions between human T and B cells were insufficient to activate the molecular machinery responsible for the class-switch recombination (CSR) of B cells.

Successful reconstitution of human autoimmunity by transferring patient-derived PBMCs into experimental mice has been

Correspondence: Dr. Takashi Usui
e-mail: takausui@kuhp.kyoto-u.ac.jp

reported [13]. However, to our knowledge, there are no studies that have focused on the reconstitution of human autoimmunity using NOG/NSG mice. In addition, transferring PBMCs often causes lethal GVH disease (GVHD) in these mice, which makes long-term engraftment of human PBMCs and reconstitution of human immune systems difficult.

In the present study, we successfully engrafted PBMC-derived $CD45RO^+CD4^+$ memory T (Tm) and B cells obtained from adult humans into NSG mice without lethal GVHD. Subsequently, all isotypes of human Igs were produced de novo in these mice, which could be attributed to the interactions between the transferred Tm and B cells. We also transferred Tm and B cells obtained from patients with rheumatoid arthritis (RA) or antisynthetase syndrome into NSG mice and observed that sustained production of IgM-rheumatoid factor (RF) as well as antiaminoacyl-tRNA synthetase (ARS) Abs in these mice. These results suggest that the selective transfer of PBMC-derived Tm and B cells into these mice could be a useful method for the study of human autoimmune mechanisms.

Results

Removal of naïve T cells from donor PBMCs prevents GVHD-associated death in engrafted NSG mice

Because GVHD is a major issue that severely restricts the observation period in NSG mice after human PBMC-derived lymphocytes transfer, we first compared several conditions for the effective engraftment of human PBMCs. We prepared PBMC subfractions, whole PBMCs, naïve $CD4^+$ T (Tn) cells, or Tm cells obtained from healthy donors. Cells of each subfraction were injected into NSG mice at 1×10^6 per mouse, and we compared the severity of GVHD among the groups. As shown in Figure 1A and B, the mice that received whole PBMCs or Tn cells lost body weight dramatically from approximately day 40 posttransfer, and did not survive beyond day 50 posttransfer. However, the mice that received Tm cells, despite showing mild GVHD that was histologically characterized by scattered or cluster-forming perivascular infiltration of human $CD45^+$ cells in the affected organs (Fig. 1C), did not lose body weight and survived longer than the other two groups. The percentage of human $CD45^+$ cells in the total mouse mononuclear cells (% hCD45) in the peripheral blood (PB) tended to increase more significantly in whole PBMC- or Tn-cell-transferred mice than in Tm-cell-transferred mice prior to death. In the Tm-cell-transferred group, the percent human CD45 continued to increase until approximately day 50 posttransfer and gradually decreased to low plateau levels; however, human $CD45^+$ cells were still detectable on day 150 posttransfer (Fig. 1D, left). In addition, FACS analysis showed a significant difference in the % hCD45 between the spleen and PB or BM in the terminal stages (days 180–250 posttransfer), which indicated that the transferred Tm cells had almost disappeared from the PB or BM but had preferentially resided in the spleen (Fig. 1D, right). We further fractionated the Tm cells into central memory T cell and effector memory T-cell fractions and compared posttransfer changes, which showed no differences in body weight changes, survival, and serial changes in the % hCD45 in the PB from those of the Tm-cell-transferred mice (data not shown). Taken together, these results show that GVHD-associated death was avoidable by removing the Tn-cell fraction from the donor PBMCs.

Transferred Tm cells are functionally competent and can act as APCs

Because the diversity of the TCR repertoire is necessary for appropriate specific immune responses, we tested whether the transferred Tm cells had retained the diversity of the TCR repertoire in the engrafted mice. We performed spectratyping of CDR3 in the TCRβ chains and compared the diversity between the Tn and Tm cells, both of which were freshly obtained from PBMCs from the same donors as the transferred Tm cells and the Tm cells collected from the spleens of NSG mice on day 230 posttransfer. Though less diverse than T cells freshly obtained from the donors, the mouse-derived Tm cells still showed CDR3 diversity despite the passing of a significant amount of time after the transfer (Fig. 2A). We next performed intracellular cytokine staining (ICS) to test the cytokine secretion of the Tm cells collected from the PB of the engrafted mice on day 100 posttransfer and found that the transferred Tm cells could secrete significant levels of IFN-γ, IL-17, and IL-21 (Fig. 2B). We further measured human *IL-21* mRNAs in the Tm cells purified from the spleens and PB of the NSG mice on day 200 posttransfer as well as in freshly prepared Tn and Tm cells obtained from PBMCs of the same human donors. Interestingly, only the Tm cells in the spleens of the engrafted mice significantly expressed human *IL-21* mRNAs (Fig. 2C). This result indicated that the transferred Tm cells were constitutively activated and expressed high levels of IL-21 in the mouse spleen. We further tested whether the surface phenotypes of the Tm cells had changed after the transfer. In addition to the conventional markers, all the Tm cells collected from the mouse spleens on day 200 posttransfer expressed HLA-DR molecules, while most of the freshly isolated human PBMC-derived Tm cells did not (Fig. 2D). Although mouse T cells do not normally express MHC class II molecules, most other species including humans do; thus, activated T cells can also act as APCs [14]. All these results suggested that most of the transferred Tm cells eventually subsided in the spleen without circulating in the PB long after the transfer and were constitutively activated to interact with other cells through both contact dependent and independent mechanisms.

Human B cells are efficiently engrafted into NSG mice by sequential transfer after Tm cells

Because IL-21 is important for B-cell maturation [15], the result that the transferred Tm cells constitutively produced abundant human IL-21 in the spleens of Tm-cell-engrafted NSG mice was

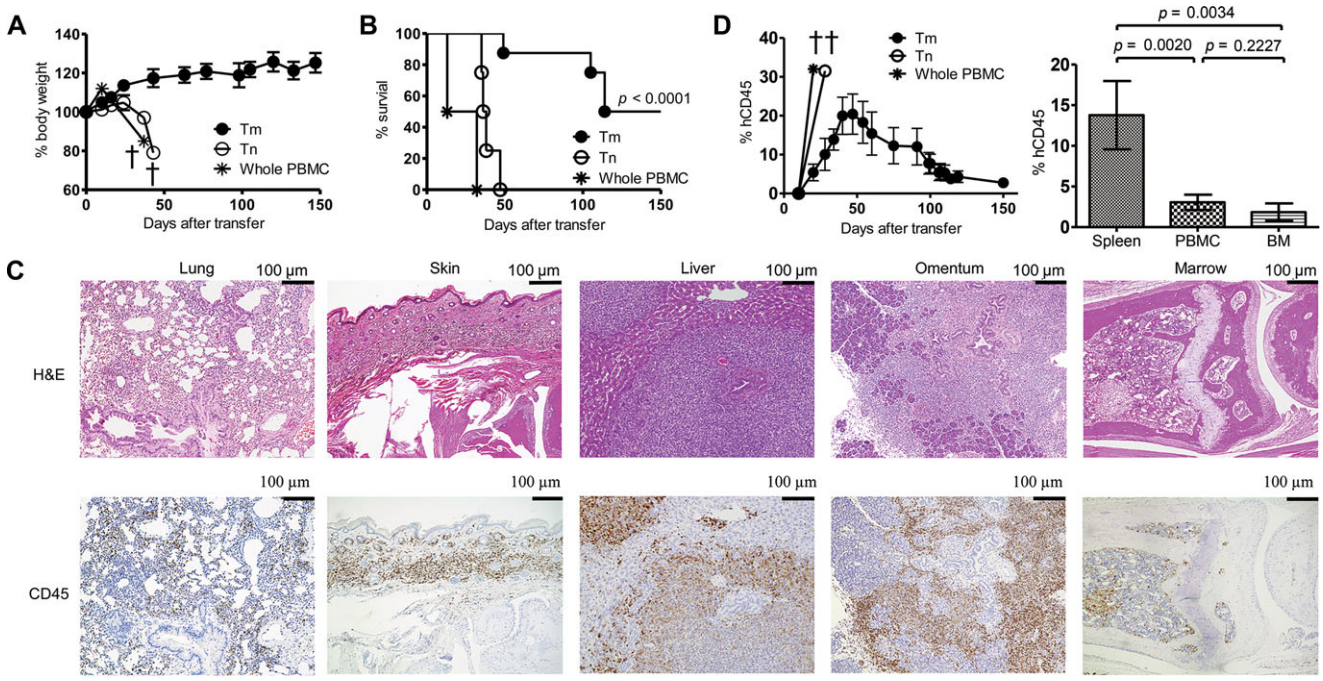

Figure 1. Lethal GVH disease is preventable by removing naïve T cells from donor PBMCs. One million whole human PBMCs ($n = 3$), human $CD45RA^+CD4^+$ naïve T (Tn) cells ($n = 4$), or $CD45RO^+CD4^+$ memory T (Tm) cells ($n = 8$) per mouse were prepared and transferred into NSG mice (day 0). (A) Serial percent changes in body weight, and (B) percent survival were assessed on the indicated days. The data in (A) are shown as mean ± SEM of the indicated number of mice, each considered its own experiment, and the data are pooled. A log-rank test was used in (B). (C) Histopathological analysis was performed to assess changes associated with mild GVH disease in the organs of Tm-cell-transferred mice on day 150 posttransfer. Specimens were stained with H&E (upper panels) or immunohistochemically stained with an anti-human CD45 Ab (lower panels). Images are representatives of eight independent experiments. (D) The percentage of human $CD45^+$ cells in total mouse mononuclear cells (% hCD45) was determined by FACS in the indicated groups of mice at 7-day intervals (left). The % hCD45 in the spleen, PBMC, and BM of the Tm cell-engrafted mice was assessed by FACS on day 150 post-Tm-cell transfer (right). After the live lymphocytes were gated, the percentages of human or mouse $CD45^+$ cells were determined by FACS. † Indicates the death of all mice within a group. The data are shown as mean ± SEM of five mice for each group from a single experiment representative of three independent experiments. The p value was determined using a Mann–Whitney U-test.

thought to be favorable for human B-cell engraftment. Thus, we hypothesized that sequential transfer of Tm and B cells could lead to effective engraftment of both cell populations. Furthermore, effective T- and B-cell interactions could induce specific immune responses with appropriate Ag stimulation. We purified PBMC-derived B cells from the same Tm-cell donor and transferred 0.5×10^6 of the B cells per mouse into the NSG mice 60 days after the transfer of 1×10^6 Tm cells per mouse. In that period, the % hCD45 in the mouse PBMCs was at a low plateau level. Interestingly, all human Ig isotypes began to increase dramatically as early as day 7 post-B-cell transfer and continued to increase, reaching approximately one-fifth of the levels observed in humans (Fig. 3A, white circles). Among the IgG subclasses, IgG3 was the most abundant followed by IgG1, while IgG2 and IgG4 were relatively suppressed, which was different from the pattern observed in healthy humans [16] (Fig. 3B). We also transferred allogeneic B cells, and compared the Ig production with an autologous B-cell transfer; the mice that received autologous B cells showed faster and greater human Ig production (Fig. 3C). In addition, IgE production was highly restricted in the allogeneic B-cell-transferred mice.

Interestingly, the % hCD45 in mouse PBMCs was transiently re-elevated at approximately 20–30 days after the B-cell transfer in both the autologous and allogeneic B-cell-transferred mice (Fig. 3D, left). Transferred B cells were initially detected in the PB (Fig. 3D, right); however, they gradually decreased and disappeared from the mouse PB (data not shown). On the other hand, plasma levels of human Igs remained at peak levels during the observation period. These results strongly suggested that like transferred Tm cells, transferred B cells also survived in the mouse spleen, and continued to produce large amounts of human Ig.

B cells transferred into NSG mice can survive only in the presence of Tm cells

Although both Tm and B cells gradually disappeared from the systemic circulation after the transfer, histological analyses of the spleens or, in some mice, the retroperitoneal lymphoid nodules on day 200 post-T-cell transfer (day 140 post-B-cell transfer) showed massive infiltration of human $CD45^+$ cells, $CD3^+$ cells, and $CD20^+$ cells in these organs (Fig. 4A). These human lymphocytes were also detected by FACS analyses of splenocytes (Fig. 4B). In addition, $CD138^+$ plasmablasts/plasmacytes were also observed in the spleens and the lymphoid nodules (Fig. 4A). Although there was no apparent lymphoid follicle, the B cells and plasmablasts/plasmacytes formed proximal clusters with T cells

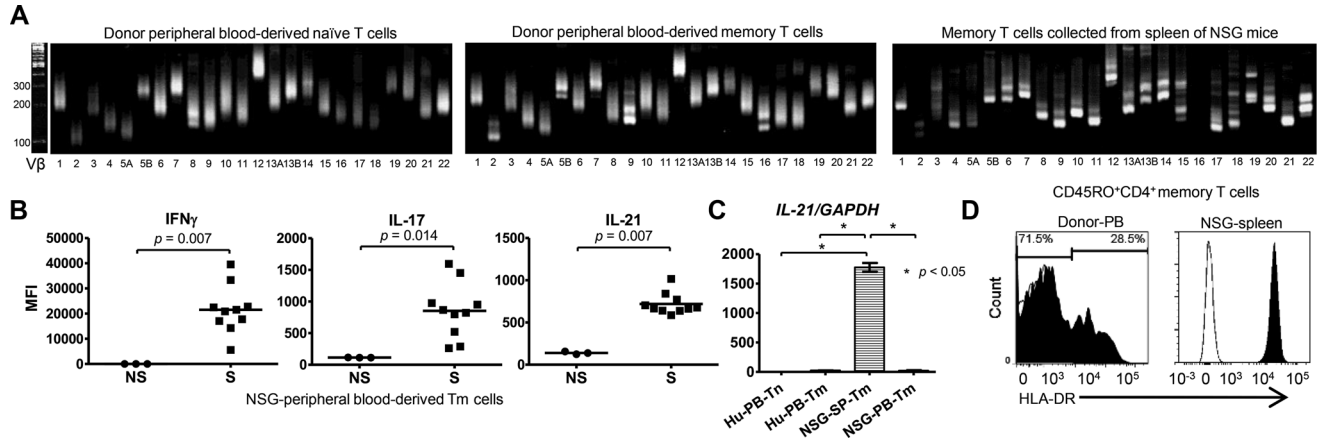

Figure 2. Transferred Tm cells are functionally competent and are able to act as APCs. One million Tm cells per mouse were transferred into NSG mice (day 0), and the engrafted Tm cells were collected from the peripheral blood (PB). (A) Representative results of three independent spectratypings of CDR3 in TCRβ chains were compared among freshly prepared Tn and Tm cells from the donor PBMCs and the same donor-derived Tm cells that were collected from the spleens of recipient NSG mice on day 230 posttransfer. (B) Tm cells collected from the PBMCs of the engrafted mice on day 100 posttransfer were stimulated with 20 ng/mL PMA and 1 μM ionomycin, and IL-17, IL-21, and IFN-γ production was evaluated by intracellular cytokine staining. S: stimulated conditions ($n = 10$); NS: nonstimulated conditions ($n = 3$); MFI: mean florescent intensity. Each symbol represents a single mouse and the mean values are indicated by horizontal bars; data are from the indicated numbers of independent mice, each considered own its experiment. A Mann–Whitney *U*-test was used for comparison. (C) Human *IL-21* mRNA expression, as assessed by quantitative PCR, was compared among donor PBMC-derived fresh Tm (Hu-PB-Tm) or Tn cells (Hu-PB-Tn) and mouse spleen-derived Tm cells (NSG-SP-Tm) or mouse PBMC-derived Tm cells (NSG-PB-Tm). Values normalized to *GAPDH* are presented as the mean ± SEM of three independent experiments. The *p* value was determined using a Kruskal–Wallis test and a Shirley–Williams posthoc test. (D) HLA-DR expression, as assessed by FACS, was compared between Tm cells freshly obtained from donor PBMCs and those collected from NSG spleens on day 200 posttransfer. The data shown are representative of three independent experiments.

distributed throughout the B-cell clusters. Professional APCs, monocytes and DCs, were not detected in any organs (data not shown), which ruled out the possible contamination of human APCs in the transferred cells. In the BM, some degree of T-cell infiltration was detected; however, B-cell infiltration was scarce and plasmablasts/plasmacytes were not detected in any of the mice (data not shown). To confirm the requirement for T-cell help for the B-cell engraftment, we transferred 0.5×10^6 purified B cells per mouse obtained from the same donors into NSG mice without a preceding Tm-cell transfer. Neither human $CD45^+$ cells (Fig. 4C and D) nor human Ig (Fig. 3A, black dots) was detected at any time (~day 100). These results indicated that the sequential transfer of Tm and B cells into NSG mice led to the successful engraftment of both cell populations. Therefore, it was speculated that the strong and persistent T- and B-cell interactions continued to occur in the spleen and the lymphoid nodules of the engrafted mice.

B cells transferred into NSG mice undergo CSR in the lymphoid organs in the presence of Tm cells

The above results also strongly suggested that the transferred B cells were able to undergo CSR if the autologous Tm cells were co-localized in vivo. Thus, we performed histological analyses of the spleens and the lymphoid nodules obtained from NSG mice engrafted with allotype-matched Tm and B cells on day 200 post-T-cell transfer (on day 140 post-B-cell transfer); the scattered infiltration of activation-induced cytidine deaminase (AICDA) positive cells were observed in both the spleens and the lymphoid nodules (Fig. 5A). In addition, *AICDA* and *Iγ-Cμ circular transcripts (Iγ-Cμ CTs)* were obtained by RT-PCR using RNA obtained from the same spleens as described above (NSG; Fig. 5B). As was consistent with a previous report, *AICDA* mRNA was also detected in Jurkat cells [17], while *Iγ-Cμ CTs* were not. Neither *AICDA* nor *Iγ-Cμ CTs* were detected in the spleens of NSG mice that received B cells only (data not shown); freshly obtained human PBMC-derived B cells or those cultured with in the presence of CD40L, IgM, IL-21, IL-4, and LPS expressed both *AICDA* and *Iγ-Cμ CTs* (Fig. 5B). To confirm CSR of the transferred B cells, we examined the other CSR-associated products, *S_H-S_H switch circular DNA products* (*scDNAs*) [18], by nested PCR. All classes of *scDNAs*, *$Sγ_{1/2}$-Sμ*, *$Sγ_3$-Sμ*, *$Sγ_4$-Sμ*, *$Sα_{1/2}$-Sμ*, *$Sα_{1/2}$-Sγ*, *Sε-Sμ*, *Sε-Sγ*, were obtained from the spleens of the Tm- and B-cell-engrafted mice, while these products were not amplified from the spleens of the only B-cell-transferred mice or the human PBMC-derived noncultured B cells (Fig. 5C). These results indicated that the transferred B cells were able to undergo CSR in the presence of Tm cells as a result of the sustained T- and B-cell interactions in the lymphoid organs of the engrafted mice.

Human auto-Ab production is maintained after transfer of patient-derived Tm and B cells into NSG mice

Some auto-Abs are considered to have pathological roles in human autoimmune diseases [19] and to be produced by auto-reactive B-cell clones [20]. Thus, we considered whether it would be possible to maintain the production of human auto-Abs in NSG mice and to cause disease-specific pathologic changes

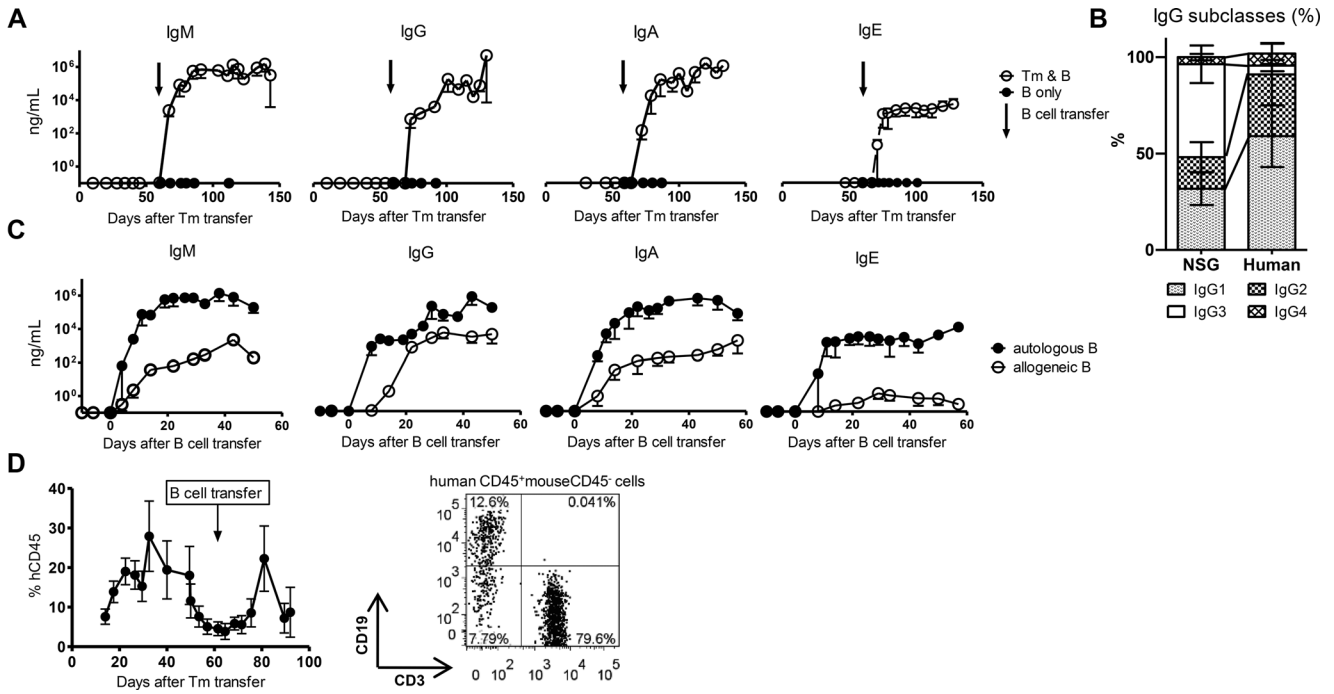

Figure 3. Human PBMC-derived B cells are efficiently engrafted by sequentially transferring them after Tm cells. NSG mice were injected intraperitoneally with 1×10^6 purified human Tm cells per mouse (day 0), and 0.5×10^6 autologous or allogeneic PBMC-derived B cells per mouse were injected into the same mice on day 60 posttransfer. (A) Serial changes in human Ig isotypes in the mouse plasma (white circles, Tm- and B-cell-transferred mice, $n = 20$; black dots, only B-cell-transferred mice, $n = 10$) were assessed by ELISA. The timing of B-cell transfers is indicated by arrows and arranged between the groups. Data are shown as mean ± SEM of the indicated numbers of mice, each evaluated in its own experiment, and the data are pooled. (B) The ratios of human IgG subclasses in the sera of Tm- and B-cell-engrafted NSG mice (day 100 posttransfer) and in healthy human sera were compared by ELISA. Data shown are from 20 independent experiments and shown as mean ± SEM in (B). (C) Serial changes in human Ig isotypes in mouse plasma were compared between the mice that received autologous B cells ($n = 20$) and the mice that received allogeneic B cells ($n = 10$) by ELISA. Data are shown as mean ± SEM of the indicated numbers of mice, each evaluated in its own experiment, and the data are pooled. (D) Serial changes in human CD45 expression in PBMCs were assessed by FACS and are shown as mean ± SEM in left. A representative dot plot of mouse PBMCs 20 days after B-cell transfer is presented on the right. Data shown are from a single experiment representative of 30 independent experiments performed.

by the transfer of PBMC-derived Tm and B cells obtained from patients with autoimmune diseases. We enrolled RA patients with IgM-RF and patients with antisynthetase syndrome, including a polymyositis patient with antihistidyl-tRNA synthetase (Jo-1) Ab and a dermatomyositis patient with antiglycyl-tRNA synthetase (EJ) Ab because corresponding Ags of these auto-Abs were thought to be highly homologous with those of mice, and these auto-Abs themselves may be pathological [21, 22]. All the mice survived during the observation period (17 weeks), and the % hCD45 in the mouse PBMCs changed in the same manner as observed in the healthy donor-derived Tm- and B-cell-transferred mice (data not shown). Interestingly, plasma levels of IgM-RF were gradually increased immediately after the transfer in the mice engrafted with Tm and B cells derived from RA patients (Fig. 6A, right), while IgM-RF was not detectable in the mice engrafted with Tm and B cells derived from patients with antisynthetase syndrome (Fig. 6A, left). On the other hand, both IgG-anti-ARS Abs, anti-Jo-1 and anti-EJ Abs, were detected only immediately after the transfer and the titer decreased to below threshold levels within a few weeks (data not shown). We also then measured IgM-anti-ARS Abs. The mice engrafted with Tm and B cells derived from patients with antisynthetase syndrome showed high levels of plasma IgM-anti-ARS Abs, and the peak values were significantly elevated compared with those of the mice engrafted with Tm and B cells derived from RA patients (Fig. 6B, left). However, in contrast with IgM-RF, the Ab-titers decreased gradually during the observation period (Fig. 6B, right). We further performed a histological analysis to investigate pathological changes; some mice engrafted with RA patient-derived Tm and B cells showed histological joint destruction, and some mice engrafted with antisynthetase syndrome patient-derived Tm and B cells showed minute infiltration of human lymphocytes in the leg muscle (Supporting Information Fig. 1). However, these findings were not consistent through the engrafted mice and were difficult to distinguish from the changes detected in chronic GVHD. Taken together, these results indicated that the production of some types of human auto-Abs, especially IgM-Abs, can be maintained in NSG mice by transferring patient-derived Tm and B cells.

Discussion

We sequentially transferred human PBMC-derived Tm and B cells into NSG mice and achieved functional engraftment of these cells. Although lethal GVHD is a major problem in using PBMCs as

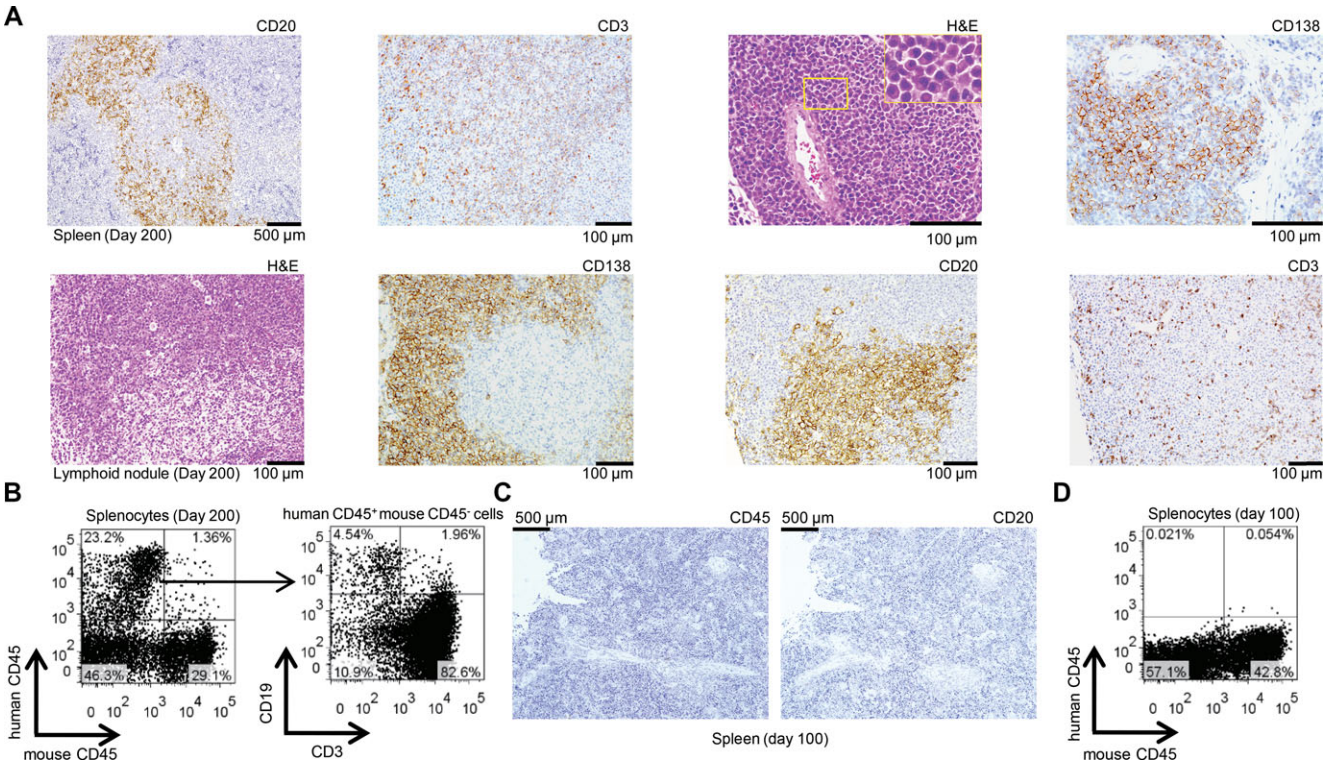

Figure 4. Transferred human B cells can survive only in the presence of human Tm cells in NSG mice. (A) Histological analysis of spleens and lymphoid nodules of Tm- and B-cell-engrafted NSG mice was performed on day 200 post-Tm-cell transfer. The specimens were stained with H&E or immunohistochemically stained with the indicated anti-human Abs. Images are representative of 30 mice. (B) The presence of human lymphocytes in the mouse splenocytes on day 200 posttransfer was analyzed by FACS. Plots are representative of 20 mice. (C and D) NSG mice ($n = 10$) were injected intraperitoneally with 0.5×10^6 B cells purified from PBMCs of healthy donors (day 0) per mouse without a preceding Tm-cell transfer. Immunohistochemical analysis of the spleens stained with anti-human CD45 and anti-human CD20 Abs and FACS analysis examining CD45 expression on splenocytes were performed on day 100 posttransfer. The data are representative of ten mice.

sources of grafts, we were able to avoid this by simply removing the Tn-cell fraction from the donor PBMCs. Because Ag-specific pathological T cells should be in the Tm-cell fraction and an aberrant or skewed T-cell population has also been observed in the Tm-cell fraction in various human autoimmune diseases such as RA [23], our strategy had advantages to increase the chance for selective expansion of pathological T cells in engrafted mice.

Although both transferred Tm and B cells gradually disappeared from the PB after the transfer, they resided in the spleen and the lymphoid nodules and survived for several months. Interestingly, histological study of the lymphoid nodules of Tm- and B-cell-transferred mice revealed a characteristic distribution of T cells, B cells, and plasma cells (Fig. 4A): T cells were distributed in a scattered manner, B cells formed clusters, and plasmablasts/plasmacytes localized just outside the B-cell clusters. This characteristic cell distribution was similar to that of the secondary lymphoid organ and indicated the interactions among these cells. On the other hand, plasmacytes were not detected in the BMs and most of the infiltrating cells were $CD4^+$ T cells. We also sequentially transferred Tm and naïve B cells instead of total B cells. However, it was technically difficult to obtain sufficient naïve B cells due to their adherent properties, and transferred naïve B cells failed to engraft (data not shown). Although we acknowledge the absence of definitive evidence of an interaction between the transferred Tm and B cells, the data presented in this study are convincing. First, the transferred B cells were not maintained without a preceding Tm-cell transfer, while they were well maintained in the presence of the engrafted Tm cells. Second, transferred B cells underwent de novo CSR, which resulted in the production of all isotypes of human Ig at significant levels. Third, allotype-matched Tm- and B-cell transfers resulted in significant and more rapid human Ig production than that observed in the case of allotype-unmatched transfers. Fourth, because human IL-21 strongly induces IgG1- and IgG3-producing CSR in concert with CD40-CD40L interactions [24], the observation that the transferred Tm cells constitutively secreted high amount of IL-21 in the spleen might explain why IgG3 was the dominant subclass of IgG in the engrafted mouse. Fifth, professional APCs were not detected in the mice; rather, transferred Tm cells expressed HLA-DR molecules and maintained TCR diversity even 7– 8 months after the transfer, which suggested that activated Tm cells also acted as APCs in the engrafted mouse. All these data strongly suggested that the strong and persistent interaction between the transferred Tm and B cells resulted in the reconstruction and the persistence of this quasi-human immune system in the engrafted mice. However, to obtain definitive evidence of T-cell-dependent B-cell differentiation and specific Ab production in these mice, immunization studies using appropriate Ags need to be performed.

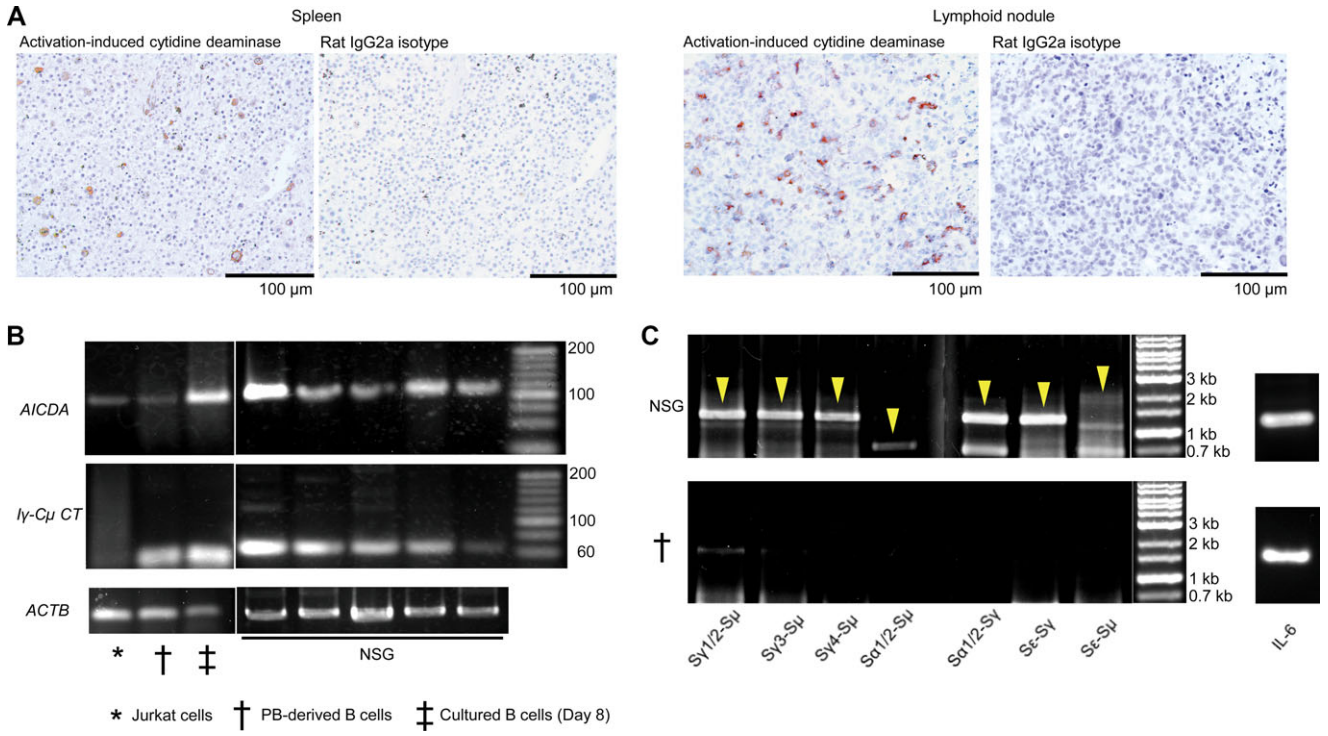

Figure 5. Transferred B cells undergo CSR in lymphoid organs of engrafted mice. (A) Spleens (left panels) and lymphoid nodules (right panels) obtained on day 200 post-Tm-cell transfer were immunohistochemically stained with anti-human activation-induced cytidine deaminase Ab and its isotype control. Images are representative of ten independent experiments. (B and C) Total RNA and genomic DNA were obtained from mouse spleens (NSG) on day 200 post-Tm-cell transfer. (B) The expression of *activation-induced cytidine deaminase* (*AICDA*), and *Iγ-Cμ circular transcripts* (*Iγ-Cμ CT*) was compared among the indicated samples by RT-PCR. (C) Nested PCR was performed to amplify the S_H-S_H *switch circular DNAs* from genomic DNA. Objective bands are indicated by yellow arrow heads. Beta actin (*ACTB*) in RT-PCR and *IL-6* in nested PCR were used as internal controls, respectively. Total RNA obtained from Jurkat cells (*), and total RNA and genomic DNA obtained from day 0 (†) or day 8 (‡) cultured $CD20^+$ B cells as described in *Material and methods* were also examined for comparison. (B and C) The presented data are representative of ten independent experiments.

Based on these findings, we tried to induce Ag-specific auto-Ab production in NSG mice using PBMCs obtained from autoimmune-disease patients. Transferring PBMC-derived Tm and B cells obtained from RA patients with IgM-RF led to the sustained production of IgM-RF in the transferred mice, and the titers continued to increase during the observation period, which was not observed in the case of transfer of Tm and B cells obtained from IgM-RF negative patients. Because corresponding IgM-RF Ags are IgG Fc fragments or denatured IgG molecules [25], which were continuously supplied by the transferred B cells, it is reasonable that

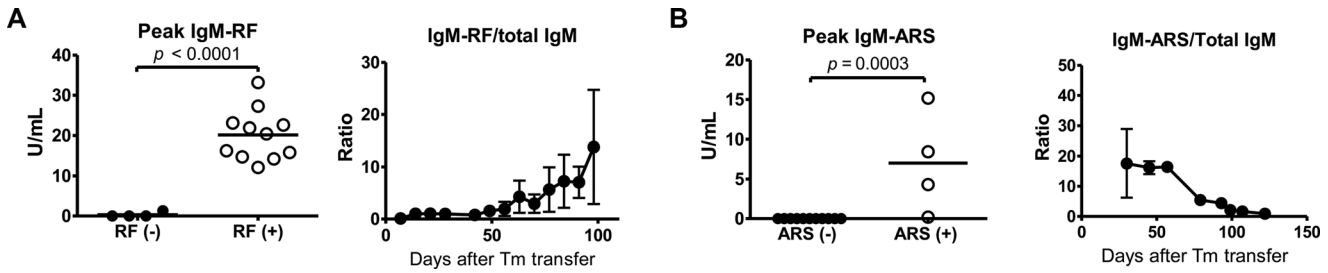

Figure 6. Auto-Ab production is maintained after transferring PBMCs from patients with autoimmune diseases. NSG mice were injected with 1×10^6 Tm cells and 0.5×10^6 B cells obtained from PBMCs of the patients with rheumatoid arthritis (RA) or antisynthetase syndrome per mouse. IgM-rheumatoid factor (RF) was measured by latex agglutination, and antiaminoacyl-transfer RNA synthetase (ARS) Ab was measured by ELISA. (A) Peak values (day 100 posttransfer) of IgM-RF in the mouse plasma were compared between the mice that received PBMCs from RA patients with IgM-RF ($n = 11$) and the mice that received PBMCs from patients without IgM-RF ($n = 4$), and serial changes in plasma IgM-RF/total IgM ratio are presented (right). (B) Peak values (day 30 posttransfer) of plasma IgM-anti-ARS Ab in the mice that received PBMCs obtained from patients with antisynthetase syndrome ($n = 4$) or from patients with RA ($n = 11$), and serial changes in plasma IgM-ARS Ab/total IgM ratio are presented. (A and B) The data are shown as the mean or mean ± SEM of the indicated number of mice, each evaluated in its own experiment. A Mann–Whitney *U*-test was used for two-group comparisons.

IgM-RF-producing B-cell clones were maintained in the presence of Ag-specific Tm cells in these mice. On the other hand, IgG- and IgM-anti-ARS Abs were only transiently detected after the transfer of Tm and B cells derived from PBMCs of patients with antisynthetase syndrome, and the titers were gradually decreased to below the threshold levels of measurement. This might be attributable to the absence of corresponding Ags despite myositis-specific Ags; notably ARS shows high homology between human and mice. It is also known that the Ab responses against Jo-1 show remarkable species specificity [26]. Thus, it is speculated that the minute differences in the Ag-epitopes between mice and humans resulted in a failure of the persistent interaction between human ARS-specific Tm and B cells. The absence of long-lived plasmacytes in the BMs of the engrafted mice might also explain the inadequate production of anti-ARS Abs.

Successful engraftment and the induction of Ag-specific humoral immune responses using HLA-DR Tg/mouse MHC class II KO NOG mice in combination with HSC transplant has also been reported [27]. However, the Ag-specific IgG production was poor, and the T-cell functions in vitro were greatly impaired. In addition, because the emergence of pathological autoimmune cells is known to be induced by a malfunction of peripheral tolerance, but not by central tolerance [28], HSC transfer will not be able to reconstitute the same autoimmunity as donor patients in these mice. Therefore, it is possible that PBMCs are more suitable grafts for the reconstitution of human autoimmune systems in these mice.

Several groups have reported mouse models of human immune diseases, such as systemic lupus erythematosus, antiphospholipid syndrome [13], ulcerative colitis [29], or Stevens-Johnson/toxic epidermal syndrome [30] using patient-derived PBMCs. In systemic lupus erythematosus and antiphospholipid syndrome models, PBMC-transferred BALB-RAG-2$^{-/-}$IL-2R$^{-/-}$ mice showed anti-DNA Ab production in the sera and presented human disease-like lesions, such as nephritis or multiple thrombi. In ulcerative colitis or Stevens-Johnson/toxic epidermal syndrome models, PBMC-transferred NOG mice were challenged with specific Ags and subsequently developed human disease-like lesions. These models are thought to be valuable because they provide patient-specific disease models and because the same pathologies the donor patients experience are induced in the mice using patients-derived PBMCs. However, careful validation of Ag specificity or a clear distinction between the induced immunological pathology and chronic GVHD is necessary.

The mechanisms of production or pathogenic roles of many auto-Abs, including RF, have yet to be determined. Recently, unique mechanisms of RF production in association with IgG-heavy chain presented by certain HLA-DR molecules have been suggested [31]. Because IgM-RF production is able to be maintained in our model, our methods may provide a useful approach to clarify the precise mechanism of IgM-RF production and its pathological role.

In conclusion, we successfully reconstituted human immune systems in NSG mice using human PBMC-derived Tm and B cells and clarified important points for the effective engraftment and induction of Ag-specific immune responses. We expect to be able to establish more sophisticated human immune systems in this mouse strain using human PBMCs with further improvements.

Materials and methods

Animals

Six- to 8-week-old NSG mice were purchased from the Jackson Laboratory and maintained in our animal facility under specific pathogen-free conditions. All the animal procedures were approved by the Animal Experimental Committee of Kyoto University (MedKyo 12120).

Preparation of human PBMCs

PBMCs were separated from the PB of healthy donors or patients with autoimmune diseases using Lymphocyte Separation Solution (Nacalai) by density centrifugation. Human CD45RA$^+$CD4$^+$ Tn cells or CD45RO$^+$CD4$^+$ Tm cells were purified by positive selection using anti-CD45RA or anti-CD45RO MicroBeads followed by negative selection using anti-CD20 MicroBeads and finally sorted by FACS Aria II (BD Bioscience) using anti-CD4-allophycocyanin (BioLegend), anti-CD8a-FITC (BioLegend), and anti-CD19-phycoerythrin (PE; eBioscience). Central memory T cells or effector memory T cells were isolated using a CD4$^+$ Central or Effector Memory T Cell Isolation MicroBeads Kit and purified by FACS Aria II as described above. Human B cells were obtained and purified from the same or different donors as the Tm cells by negative selection using anti-human CD2 MicroBeads followed by sorting with FACS Aria II using anti-CD45-Pacific blue (eBioscience), anti-CD19-biotin detected by streptavidin-allophycocyanin/Cy7 (eBioscience), and anti-CD3-PE/Cy7 (BioLegend). The postsort purities of the CD45RA$^+$CD4$^+$, CD45RO$^+$CD4$^+$, CD45RO$^+$CD4$^+$CCR7$^+$, CD45RO$^+$CD4$^+$CCR7$^-$, and CD19$^+$ cells were >99%, and the obtained cells were injected intraperitoneally into NSG mice. The number of injected whole PBMCs or T cells was 1×10^6 per mouse, and the number of B cells was 0.5×10^6 per mouse. All MicroBeads used in the study were purchased from Miltenyi Biotec.

All the donors were adults who had provided written informed consent. The study was approved by the Institutional Review Board of the Graduate School of Medicine, Kyoto University and Kyoto University Hospital. All the patients had active disease and had high serum titers of disease-associated auto-Abs.

Flow cytometry

PB was taken from the mouse tail vein at 7-day intervals after the transfer, and plasma and blood cells were separated by density centrifugation. Single-cell suspensions were prepared from the mouse spleens and PBMCs after red

blood cell lysis with ammonium-chloride-potassium buffer. Lymphocytes were stained with anti-mouse CD45-biotin (eBioscience) and detected by streptavidin-allophycocyanin/Cy7 and the following anti-human Abs: anti-CD45-Pacific Blue, anti-human leukocyte Ag HLA-DR-biotin (BioLegend) detected by streptavidin-allophycocyanin/Cy7, anti-CD3-PE/Cy7, anti-CD4-allophycocyanin, anti-CD8a-FITC, and anti-CD19-PE. The surface markers were analyzed by FACS LSR Fortessa (BD Bioscience), and the data were analyzed using FlowJo (Tree Star).

For ICS, Tm cells were isolated from the PBMCs of Tm-cell-engrafted mice on day 100 posttransfer by positive selection using human memory $CD4^+$ T-cell isolation Microbeads. The cells were stimulated with 20 ng/mL PMA and 1 μM ionomycin for 5 h and ICS was performed as described previously [32] using anti-human-IFN-γ-allophycocyanin (eBioscience), anti-human-IL-17-FITC (eBioscience), and anti-human-IL-21-biotin (BioLegend) detected by streptavidin-allophycocyanin/Cy7. Surface markers were also co-stained as described above.

ELISA

Human Igs and IgG subclasses in the mouse plasma and human IL-21 in the mouse spleens and plasma were measured using ELISA kits (Bethyl Laboratories, Life Technologies, eBioscience) according to the manufacturers' instructions.

Human auto-Abs in mouse plasma

IgM-RF was measured using a latex agglutination kit (Sysmex). IgG-anti-ARS Abs, which includes anti-Jo-1 Ab and anti- EJ Ab, were measured using ELISA kits (MBL) [33]. IgM-anti-ARS Abs were measured by performing an ELISA using anti-human IgM Abs (Bethyl Laboratories) as detection Abs.

Histology

Paraformaldehyde-fixed paraffin-embedded sections were stained with H&E. After treatment with heated citrate buffer for Ag retrieval, immunohistochemical staining was performed with mouse anti-human-CD45, mouse anti-human CD20 (Dako), mouse anti-human-CD3 (Leica Biosystems), mouse anti-human-CD138 (Nichirei Biosciences) Abs, and corresponding HRP-conjugated anti-mouse IgG isotypes (Dako). Some specimens were also immunohistochemically stained with a rat anti-human-AICDA Ab and an HRP-conjugated rat IgG2a kappa isotype control (eBioscience).

Cell culture

Human B cells were obtained from the PBMCs of healthy donors by positive selection using anti-human-CD20 MicroBeads. Twelve-well culture plates were pretreated with 1 μg/mL anti-human CD40L (eBioscience) and 1 μg/mL anti-human-IgM Ab (BioLegend). One million cells per well were cultured in 1 mL RPMI-1640 complete medium (Gibco) in the presence of 20 ng/mL IL-21 (Cell Signaling Technology), 10 ng/mL IL-4 (Life Technologies), and 10 ng/mL LPS (Sigma-Aldrich) at 37°C in a 5% CO_2 incubator [18]. To confirm CSR of the cultured B cells, we assessed the surface markers on sequential days from days 0 to 8 using anti-CD3-PE/Cy7, anti-CD138-FITC (BioLegend), and anti-CD19-biotin detected by streptavidin-allophycocyanin/Cy7 and determined that the cells on day 8 were the most enriched for $CD19^{\pm}CD138^+$ plasmablasts/plasmacytes. After the cells were collected on day 8, total RNA and genomic DNA were extracted using ISOGEN (Nippon Gene) and DNeasy (Qiagen) kits, respectively. The obtained RNA was treated with TURBO™ DNase (Life Technologies) and, purified with an RNeasy Mini Kit (Qiagen).

PCR

RT-PCR was performed as follows. After isolation and purification of total RNA obtained from mouse spleens or PBMCs, first-strand complementary DNA was synthesized using Superscript III Reverse Transcriptase and random primers (Life Technologies). The synthesized first-strand complementary DNA was amplified using a Mastercycler ep (Eppendorf), with iProof™ High-Fidelity DNA Polymerase (BioRad) for *beta actin*, *AICDA*, and *Iγ-Cμ CTs* using gene-specific primers. Real-time PCR was performed in a Light Cycler 480 (Roche Applied Science) using universal probe library sets for human and gene-specific primers for *IL-21* and *GAPDH*. Genomic DNA was also isolated using a DNeasy kit, and S_H-S_H *scDNAs* were amplified by nested PCR as described previously [18]; a human-IL-6 gene locus was amplified as a positive control. We used Jurkat cells (RIKEN, Bio-Resource Center) as a non-B-cell control. For a CSR positive control, we used human PBMC-derived B cells cultured as described above. Genomic DNA obtained from freshly isolated human PBMC-derived B cells was used as a negative control.

To analyze the TCR repertoire diversity, we performed spectratyping of CDR3 in TCRβ chains by nested PCR as described previously [34] after obtaining genomic DNA from the Tm and Tn cells freshly isolated from the PBMC donor, and the Tm cells collected from NSG spleens on day 230 posttransfer. Primer pairs used in this study are listed in Supporting Information Table 1.

DNA cloning and sequencing

PCR products or DNA bands purified from agarose gels were cloned using Zero Blunt PCR Cloning Kits (Life Technologies). Plasmids were isolated using a QIAprep Miniprep kit (Qiagen), and DNA sequencing was performed on a 3130xl Genetic Analyzer using a BigDye Terminator v3.1 Cycle Sequencing Kit (Applied Biosystems).

Statistical analysis

A Mann–Whitney *U*-test was used for two-group comparisons, Kruskal–Wallis and Shirley–Williams posthoc tests were used for multiple group comparisons, and the log-rank test was used for the comparison of survival curves. Error bars in all the figures indicate the SEM. p values < 0.05 were considered statistically significant.

Acknowledgments: This work was supported by a grant-in-aid for scientific research (18591106 and 20591168 to T.U. and 18390290 and 22390201 to T.M.) from the Japan Society for the Promotion of Science. DNA sequencing analysis was performed at the Medical Research Support Center, Graduate School of Medicine, Kyoto University. We are grateful for the essential collaboration of the patients who participated in this study.

Conflict of interest: The authors declare no commercial or financial conflict of interest.

References

1 **Bosma, G. C., Custer, R. P. and Bosma, M. J.**, A severe combined immunodeficiency mutation in the mouse. *Nature* 1983. **301**: 527–530.

2 **Ohbo, K., Suda, T., Hashiyama, M., Mantani, A., Ikebe, M., Miyakawa, K., Moriyama, M. et al.**, Modulation of hematopoiesis in mice with a truncated mutant of the interleukin-2 receptor gamma chain. *Blood* 1996. **87**: 956–967.

3 **Pino, S., Brehm, M. A., Covassin-Barberis, L., King, M., Gott, B., Chase, T. H., Wagner, J. et al.**, Development of novel major histocompatibility complex class I and class II-deficient NOD-SCID IL2R gamma chain knockout mice for modeling human xenogeneic graft-versus-host disease. *Methods Mol. Biol.* 2010. **602**: 105–117.

4 **Nakamura, M. and Suemizu, H.**, Novel metastasis models of human cancer in NOG mice. *Curr. Top. Microbiol. Immunol.* 2008. **324**: 167–177.

5 **Hajj, H. E., Nasr, R., Kfoury, Y., Dassouki, Z., Nasser, R., Kchour, G., Hermine, O. et al.**, Animal models on HTLV-1 and related viruses: what did we learn? *Front Microbiol.* 2012. **3**: 333.

6 **Nischang, M., Sutmuller, R., Gers-Huber, G., Audigé, A., Li, D., Rochat, M. A., Baenziger, S. et al.**, Humanized mice recapitulate key features of HIV-1 infection: a novel concept using long-acting anti-retroviral drugs for treating HIV-1. *PLoS One* 2012. **7**: e38853.

7 **Kuwana, Y., Takei, M., Yajima, M., Imadome, K., Inomata, H., Shiozaki, M., Ikumi, N. et al.**, Epstein-Barr virus induces erosive arthritis in humanized mice. *PLoS One* 2011. **6**: e26630.

8 **Ishikawa, F., Yasukawa, M., Lyons, B., Yoshida, S., Miyamoto, T., Yoshimoto, G., Watanabe, T. et al.**, Development of functional human blood and immune systems in NOD/SCID/IL2 receptor {gamma} chain(null) mice. *Blood* 2005. **106**: 1565–1573.

9 **Traggiai, E., Chicha, L., Mazzucchelli, L., Bronz, L., Piffaretti, J. C., Lanzavecchia, A. and Manz, M. G.**, Development of a human adaptive immune system in cord blood cell-transplanted mice. *Science* 2004. **304**: 104–107.

10 **Covassin, L., Jangalwe, S., Jouvet, N., Laning, J., Burzenski, L., Shultz, L. D. and Brehm, M. A.**, Human immune system development and survival of NOD-scid IL2rg(null) (NSG) mice engrafted with human thymus and autologous hematopoietic stem cells. *Clin. Exp. Immunol.* 2013. **174**: 372–388.

11 **Watanabe, Y., Takahashi, T., Okajima, A., Shiokawa, M., Ishii, N., Katano, I., Ito, R. et al.**, The analysis of the functions of human B and T cells in humanized NOD/shi-scid/gammac(null) (NOG) mice (hu-HSC NOG mice). *Int. Immunol.* 2009. **21**: 843–858.

12 **Ito, R., Shiina, M., Saito, Y., Tokuda, Y., Kametani, Y. and Habu, S.**, Antigen-specific antibody production of human B cells in NOG mice reconstituted with the human immune system. *Curr. Top. Microbiol. Immunol.* 2008. **324**: 95–107.

13 **Andrade, D., Redecha, P. B., Vukelic, M., Qing, X., Perino, G., Salmon, J. E. and Koo, G. C.**, Engraftment of peripheral blood mononuclear cells from systemic lupus erythematosus and antiphospholipid syndrome patient donors into BALB-RAG-2$^{-/-}$ IL-2Rgamma$^{-/-}$ mice: a promising model for studying human disease. *Arthritis Rheum.* 2011. **63**: 2764–2773.

14 **Holling, T. M., Schooten, E. and van Den Elsen, P. J.**, Function and regulation of MHC class II molecules in T-lymphocytes: of mice and men. *Hum. Immunol.* 2004. **65**: 282–290.

15 **Berglund, L. J., Avery, D. T., Ma, C. S., Moens, L., Deenick, E. K., Bustamante, J., Boisson-Dupuis, S. et al.**, IL-21 signalling via STAT3 primes human naive B cells to respond to IL-2 to enhance their differentiation into plasmablasts. *Blood* 2013. **122**: 3940–3950.

16 **Oxelius, V. A. and Pandey, J. P.**, Human immunoglobulin constant heavy G chain (IGHG) (Fcg) (GM) genes, defining innate variants of IgG molecules and B cells, have impact on disease and therapy. *Clin. Immunol.* 2013. **149**: 475–486.

17 **Qin, H., Suzuki, K., Nakata, M., Chikuma, S., Izumi, N., Huong, L. T., Maruya, M. et al.**, Activation-induced cytidine deaminase expression in CD4+ T cells is associated with a unique IL-10-producing subset that increases with age. *PLoS One* 2011. **6**: e29141.

18 **Cerutti, A., Zan, H., Schaffer, A., Bergsagel, L., Harindranath, N., Max, E. E. and Casali, P.**, CD40 ligand and appropriate cytokines induce switching to IgG, IgA, and IgE and coordinated germinal center and plasmacytoid phenotypic differentiation in a human monoclonal IgM+IgD+ B cell line. *J. Immunol.* 1998. **160**: 2145–2157.

19 **Mimori, T.**, Mechanisms of production and pathogenesis of autoantibodies. *Rinsho Shinkeigaku* 2007. **47**: 855–857.

20 **Tobón, G. J., Izquierdo, J. H. and Cañas, C. A.**, B lymphocytes: development, tolerance, and their role in autoimmunity-focus on systemic lupus erythematosus. *Autoimmune Dis.* 2013. **2013**: 827254.

21 **Mahler, M., Miller, F. W. and Fritzler, M. J.**, Idiopathic inflammatory myopathies and the anti-synthetase syndrome: a comprehensive review. *Autoimmun. Rev.* 2014. **13**: 367–371.

22 **Aletaha, D., Alasti, F. and Smolen, J. S.**, Rheumatoid factor determines structural progression of rheumatoid arthritis dependent and independent of disease activity. *Ann. Rheum. Dis.* 2013. **72**: 875–880.

23 **Matsuki, F., Saegusa, J., Miyamoto, Y., Misaki, K., Miura, Y., Kurosaka, M., Kumagai, S. et al.**, CD45RA-Foxp3(high) activated/effector regulatory T cells in the CCR7+CD45RA-CD27+CD28+central memory subset are decreased in peripheral blood from patients with rheumatoid arthritis. *Biochem. Biophys. Res. Commun.* 2013. **438**: 778–783.

24 **Pène, J., Gauchat, J. F., Lécart, S., Drouet, E., Guglielmi, P., Boulay, V., Delwail, A. et al.**, Cutting edge: IL-21 is a switch factor for the production of IgG1 and IgG3 by human B cells. *J. Immunol.* 2004. **172**: 5154–5157.

25 **Dörner, T., Egerer, K., Feist, E. and Burmester, G. R.**, Rheumatoid factor revisited. *Curr. Opin. Rheumatol.* 2004. **16**: 246–253.

26 **Katsumata, Y.**, **Ridgway, W. M.**, **Oriss, T.**, **Gu, X.**, **Chin, D.**, **Wu, Y.**, **Fertig, N. et al.**, Species-specific immune responses generated by histidyl-tRNA synthetase immunization are associated with muscle and lung inflammation. *J. Autoimmun.* 2007. **29**: 174–186.

27 **Suzuki, M.**, **Takahashi, T.**, **Katano, I.**, **Ito, R.**, **Ito, M.**, **Harigae, H.**, **Ishii, N. et al.**, Induction of human humoral immune responses in a novel HLA-DR-expressing transgenic NOD/Shi-scid/gcnull mouse. *Int. Immunol.* 2012. **24**: 243–252.

28 **Collado, J. A.**, **Guitart, C.**, **Ciudad, M. T.**, **Alvarez, I. and Jaraquemada, D.**, The repertoires of peptides presented by MHC-II in the thymus and in peripheral tissue: a clue for autoimmunity? *Front Immunol.* 2013. **4**: 442.

29 **Nolte, T.**, **Zadeh-Khorasani, M.**, **Safarov, O.**, **Rueff, F.**, **Gülberg, V.**, **Herbach, N.**, **Wollenberg, A. et al.**, Oxazolone and ethanol induce colitis in non-obese diabetic-severe combined immunodeficiency interleukin-2Rg(null) mice engrafted with human peripheral blood mononuclear cells. *Clin. Exp. Immunol.* 2013. **172**: 349–362.

30 **Saito, N.**, **Yoshioka, N.**, **Abe, R.**, **Qiao, H.**, **Fujita, Y.**, **Hoshina, D.**, **Suto, A. et al.**, Stevens-Johnson syndrome/toxic epidermal necrolysis mouse model generated by using PBMCs and the skin of patients. *J. Allergy Clin. Immunol.* 2013. **131**: 434–441.

31 **Jin, H.**, **Arase, N.**, **Hirayasu, K.**, **Kohyama, M.**, **Suenaga, T.**, **Saito, F.**, **Tanimura, K. et al.**, Autoantibodies to IgG/HLA class II complexes are associated with rheumatoid arthritis susceptibility. *Proc. Natl. Acad. Sci. USA* 2014. **111**: 3787–3792.

32 **Koenen, H. J.**, **Fasse, E. and Joosten, I.**, IL-15 and cognate antigen successfully expand de novo-induced human antigen-specific regulatory CD4+ T cells that require antigen-specific activation for suppression. *J. Immunol.* 2003. **171**: 6431–6441.

33 **Nakashima, R.**, **Imura, Y.**, **Hosono, Y.**, **Seto, M.**, **Murakami, A.**, **Watanabe, K.**, **Handa, T. et al.**, The multicenter study of a new assay for simultaneous detection of multiple anti-aminoacyl-tRNA synthetases in myositis and interstitial pneumonia. *PLoS ONE.* 2014. **9**: e85062.

34 **Currier, J. R. and Robinson, M. A.**, Spectratype/immunoscope analysis of the expressed TCR repertoire. *Curr. Protoc. Immunol.* 2001. **172**: 5154–5157.

Abbreviations: **NSG**: NOD/LtSzscid/IL-2R$\gamma^{-/-}$ · **GVHD**: GVH disease · **Tm**: memory T · **NOG**: NOD/Shi-scid/IL-2R$\gamma^{-/-}$ · **CSR**: class-switch recombination · **RA**: rheumatoid arthritis · **RF**: rheumatoid factor · **ARS**: aminoacyl tRNA synthetase · **Tn**: naïve T · **% hCD45**: percent human CD45 · **PB**: peripheral blood · **ICS**: intracellular cytokine staining · ***AICDA***: activation-induced cytidine deaminase · ***Iγ-Cμ CTs***: *Iγ-Cμ circular transcripts* · ***scDNA***: *switch circular DNA product* · **Jo-1**: histidyl-tRNA synthetase · **EJ**: glycyl-tRNA synthetase · **PE**: phycoerythrin

Full correspondence: Dr. Takashi Usui, Department of Rheumatology and Clinical Immunology, Graduate School of Medicine, Kyoto University, 54 Shogoin-Kawaharacho, Sakyo-ku, Kyoto 606–8507, Japan
Fax: +81-75-751-4338
e-mail: takausui@kuhp.kyoto-u.ac.jp

Received: 9/4/2014
Revised: 12/7/2014
Accepted: 13/8/2014
Accepted article online: 22/8/2014

